

Linear stability of particle-laden thin films

Benjamin Cook*, Oleg Alexandrov**, and Andrea Bertozzi

Mathematics Department, University of California Los Angeles, Los Angeles, California

Abstract. Recent experiments [Zhou, Dupuy, Bertozzi, and Hosoi, Phys. Rev. Lett., 94 (2005)] of particle-laden film flow on an incline demonstrate new behavior distinct from the well-known clear fluid case, including the formation of a particle-rich ridge which can stabilize the advancing contact line with respect to “fingering” perturbations. We consider a model similar to that of Zhou et al. with the additional regularizing effect of shear-induced diffusion. A linear stability analysis demonstrates that particle settling moderately reduces the growth rate of unstable modes, while increasing the most unstable wavelength.

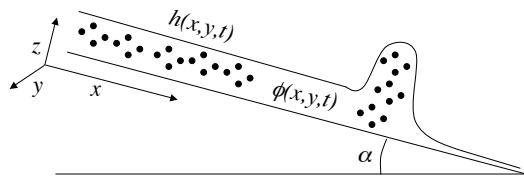


Fig. 1. The coordinate system used in this work.

iments by Zhou et al. [10] on such films have demonstrated an effect absent in liquid films: the emergence of a region near the contact line with markedly greater particle concentration and film thickness than the bulk values. This “particle-rich ridge”, due to settling of the denser particles in the down-slope direction, appeared to somewhat suppress the fingering instability in their experiments.

Zhou et al. also presented a lubrication model describing the ridge regime in terms of the film thickness h and concentration ϕ . The purpose of this work is to determine the linear stability properties of this model to compare with the corresponding liquid film [2], in order to evaluate the influence of the particle-rich ridge on the fingering instability.

We work with the dimensionless equations from [11], which corrects the velocity averaging in [10] and generalizes to two space dimensions. These equations,

$$h_t + \nabla \cdot (h \mathbf{v}_{\text{av}}) = 0, \quad (\phi h)_t + \nabla \cdot \left(\phi h \left[\mathbf{v}_{\text{av}} + (1 - \phi) \mathbf{v}_{\text{rel}} \right] \right) = 0, \quad (1)$$

involve the volume-averaged velocity of the two phases

$$\mathbf{v}_{\text{av}} = \frac{h^3}{\mu(\phi)} \nabla \nabla^2 h - D(\alpha) \left[\frac{h^3}{\mu(\phi)} \nabla(\rho(\phi)h) - \frac{5}{8} \frac{h^4}{\mu(\phi)} \nabla(\rho(\phi)) \right] + \frac{\rho(\phi)}{\mu(\phi)} h^3 \hat{\mathbf{x}}, \quad (2)$$

and the settling velocity of particles relative to the liquid

$$\mathbf{v}_{\text{rel}} = V_s f(\phi) w(h) \hat{\mathbf{x}}. \quad (3)$$

* Now at National Geospatial-Intelligence Agency, Reston, VA.

** Now at Cadence Design Systems, San Jose, CA.

The transverse fingering instability of a driven contact line has been an important research topic since it was observed by Huppert in 1982 [1], and has motivated much experimental, computational, and theoretical work [2–8]. While a similar effect has been observed in granular flows due to a different mechanism [9], the corresponding problem for particle-laden fluids has been studied only recently. Experiments

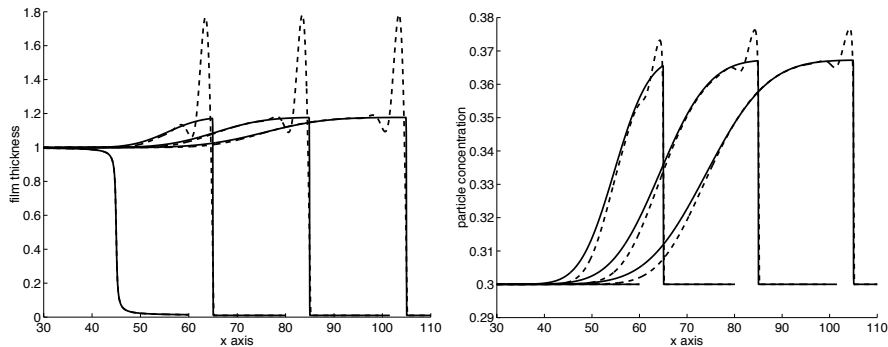


Fig. 2. The base state with $\phi_0 = 0.3$, $b = 0.01$, $\alpha = \pi/2$, obtained by a numerical solution of (1)(a), (4), (5) at times 0, 2000, 4000, and 6000. Dashed lines are smooth solutions of the full equations and solid lines are shock solutions of the reduced system. The left plot displays film thickness, the right concentration. The graphs have been shifted along the x axis to make them appear closer together.

The functions $\mu(\phi) = (1 - \phi/\phi_m)^{-2}$, $f(\phi) = (1 - \phi)^5$, $w(h) = A(h/a)^2 / \sqrt{1 + (A(h/a)^2)^2}$ with $A = 1/18$, and $\rho(\phi) = (1 + \Delta\phi)$ (representing effective viscosity, hindered settling, wall effects, and density) and the parameters $a = 0.1$, $\Delta = 1.7$, $V_s = (2/3)a^2\Delta$, $\phi_m = 0.67$, and α (representing the dimensionless particle radius, density difference, settling rate, packing fraction, and inclination angle) are explained in [10] and [11], and the nondimensional scaling and the modified capillary number $D(\alpha) = (3Ca)^{1/3} \cot \alpha$ are described in [5].

The system (1) is fourth-order, but the higher-order terms appear in (2) and not in (3), so the relative velocity is not regularized, and numerical solutions of the system (1) display an instability affecting ϕ though not h . A model derived in the appendix provides regularization in the form of shear-induced diffusion, leaving the first equation in (1) unaltered and transforming the second into

$$(\phi h)_t + \nabla \cdot \left(\phi h \left[\mathbf{v}_{\text{av}} + (1 - \phi) \mathbf{v}_{\text{rel}} \right] - \frac{3}{2} a^2 (3Ca)^{1/3} \hat{D}(\phi) \frac{h^2 \rho(\phi)}{\mu(\phi)} \nabla \phi \right) = 0. \quad (4)$$

The one-dimensional base state corresponding to a straight contact line is obtained by solving the Riemann problem for equations (1)(a) and (4), defined by the initial data

$$h(x, y, t = 0) = \begin{cases} 1 & \text{for } x < 0 \\ b & \text{for } x > 0 \end{cases}, \quad \phi(x, y, t = 0) = \phi_0, \quad (5)$$

where a precursor of thickness b is used. The precursor model requires an approximate value for b , which depends on the microscopic physics. Since this parameter is often unknown a priori, many authors present results for a range of b [2, 4]; here we refer to [11] for such a study.

Figure 2 shows simulations of both the full system and the reduced system, obtained by eliminating all terms with more than one spatial derivative. As in [10], the reduced system solution differs primarily in the lack of a capillary ridge, and is useful because it consists simply of two shock discontinuities propagating at different speeds. The well-defined region between the shocks corresponds to the particle-rich ridge, and in [11] its thickness and concentration as well as the shock speeds are determined from the Riemann data b and ϕ_0 . The fourth order terms must be included to compute the transverse instability.

In the fourth-order clear fluid problem, the base state is a single regularized shock and can be written as a traveling wave $h(x, t) = h(x - Ut)$ for an appropriate choice of U [2, 5], simplifying the stability calculation. In contrast, a double shock solution cannot be represented as a traveling wave. Following [12], we perturb the time-dependent base state

$$\bar{h}(x, y, t) = h(x, t) + \varepsilon g(x, t) \cos qy, \quad \bar{\phi}(x, y, t) = \phi(x, t) + \varepsilon \psi(x, t) \cos qy,$$

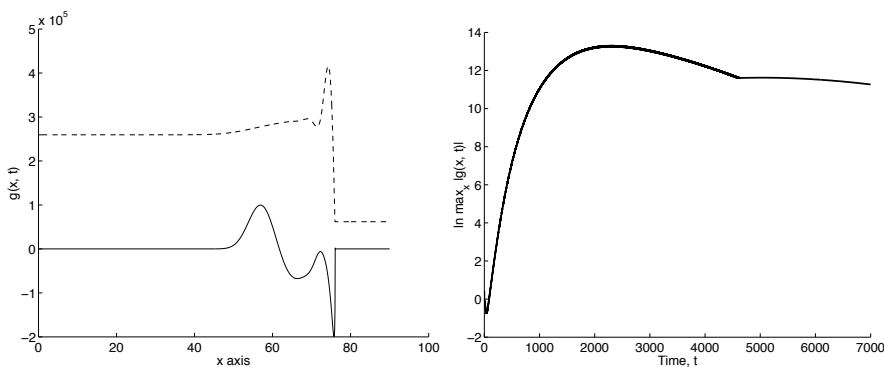


Fig. 3. On the left, the perturbation $g(t, x)$ at time $T = 4000$ for $q = 1$ (solid), with $\phi_0 = 0.3$, $b = 0.01$, $\alpha = \pi/2$. The dashed curve is $h(x, t)$ shown to illustrate the positions of the leading and trailing shocks. On the right is the decay of the perturbation in time. After a transient during which the perturbation is largest near the leading shock, the slower-decaying part at the trailing shock dominates.

and derive from (1)(a), (4) the following evolution equations for the perturbations g and ψ :

$$g_t + \left\{ h^3 \left[a(\phi) \left(g^{(3)} - q^2 g' \right) + a'(\phi) h^{(3)} \psi \right] + 3a(\phi) h^2 h^{(3)} g \right\}_x + q^2 a(\phi) h^3 (q^2 g - g'') + \left\{ h^2 [3b(\phi)g + hb'(\phi)\psi] \right\}_x = 0 \quad (6)$$

$$\begin{aligned} (\phi g + h\psi)_t + \left\{ h^3 \left[c(\phi) \left(g^{(3)} - q^2 g' \right) + c'(\phi) h^{(3)} \psi \right] + 3c(\phi) h^2 h^{(3)} g \right\}_x + q^2 c(\phi) h^3 (q^2 g - g'') \\ + \left\{ h^2 [3d(\phi)g + hd'(\phi)\psi] \right\}_x \\ + V_s \left\{ f(\phi)w(h) [\phi g + h\psi] + h\phi [\psi w(h)f'(\phi) + f(\phi)gw'(h)] \right\}_x \\ - C \left[\{p'(h)r(\phi)\phi_x g + p(h)r'(\phi)\phi_x \psi + p(h)r(\phi)\psi_x\}_x - q^2 p(h)r(\phi)\psi \right] = 0. \quad (7) \end{aligned}$$

Here we denoted $a(\phi) = 1/\mu(\phi)$, $b(\phi) = \rho(\phi)/\mu(\phi)$, $c(\phi) = \phi/\mu(\phi)$, $d(\phi) = \phi\rho(\phi)/\mu(\phi)$, $C = \frac{3}{2}a^2(3Ca)^{1/3}$, $p(h) = h^2$, $r(\phi) = \hat{D}(\phi)\rho(\phi)/\mu(\phi)$. Also, for simplicity, we assume that the film flows vertically so $\alpha = \pi/2$ and $D(\alpha) = 0$.

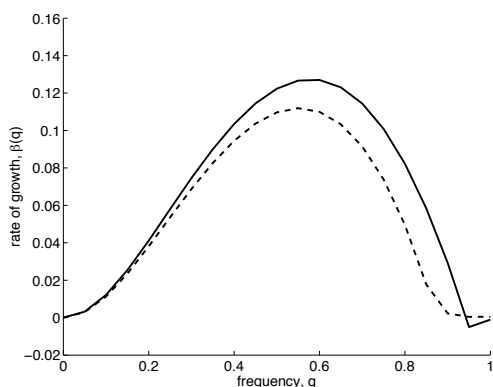


Fig. 4. The growth rate $\beta(q)$ for the film without settling (solid) and with settling (dash).

Sufficiently small perturbations will grow or decay exponentially in time, i.e. as $e^{\beta(q)t}$, corresponding to the maximum eigenvalue of each of the shocks in the composite wave. We measured the growth rate $\beta(q)$ from numerical solutions to (6)-(7) by examining the evolution of the quantity $\max_x |g(t, x)|$ in time. An example appears in figure 3.

The long time growth rates were used to infer $\beta(q)$, shown in figure 4, which like the pure fluid displays a long wave instability. Also plotted are the growth rates from calculations with V_s set to zero, which by keeping ϕ constant describe a homogeneous fluid with the same viscosity as the mixture. The effect of settling can

be seen by comparing the growth rates from these two calculations, which shows a modest reduction in the growth rate of unstable modes.

We conclude that particle settling and the resulting ridge has a moderate stabilizing effect, slowing the growth rate of the fingering instability and pushing the most unstable mode to a slightly longer wavelength. These effects were seen in the experiments of Zhou et al. [10], though it is not clear that the modest reduction in the growth rate reported here is sufficient to explain the observed effect on finger growth. We also report that the two-dimensional problem is unstable unless regularizing effects such as shear-induced diffusion are taken into account. Interesting topics for future research include the role of moderate inclination angle, non-Newtonian effects at high particle concentration, and the fully nonlinear dynamics of the model in two dimensions.

Appendix: Particle diffusion

Leighton and Acrivos [13] describe shear-induced diffusion as a concentration- and shear rate-dependent diffusion of particles with diffusivity $D = a^2\dot{\gamma}\hat{D}(\phi)$ for a suspension subject to a shear rate $\dot{\gamma}$. Experiments by Leighton [14] indicate that $\hat{D}(\phi) \approx \frac{1}{3}\phi^2 (1 + \frac{1}{2}e^{8.8\phi})$. While diffusion is strongest in the vertical (normal) direction, this effect is already incorporated in the model.¹ Here we consider the horizontal diffusion resulting from horizontal gradients of ϕ . Using dimensional variables, this particle flux appears as an extra term in equation (1):

$$(\phi h)_t + \nabla \cdot \left((\mathbf{v}_{\mathbf{av}} + \mathbf{v}_{\mathbf{rel}})\phi h - [a^2\dot{\gamma}\hat{D}(\phi)]h\nabla\phi \right) = 0. \quad (8)$$

For simplicity we consider the average vertical contribution to the shear rate $\dot{\gamma} = (1/h) \int_0^h |d\mathbf{v}_{\mathbf{av}}/dz| dz$. In smooth regions this velocity is generally dominated by its first order term, giving an average (dimensional) shear rate

$$\dot{\gamma} \approx \frac{3}{2}(g \sin \alpha) \frac{\rho(\phi)}{\mu(\phi)} h. \quad (9)$$

Substituting (9) into (8) and reverting to dimensionless variables then yields equation (4).

This work was supported by NSF grant ACI-0321917 and ONR grant N000140710431.

References

1. H.E. Huppert, *Nature* **300**, 427 (1982)
2. S. Troian, E. Herbolzheimer, S. Safran, J. Joanny, *Europhysics Letters* **10**, 25 (1989)
3. J.M. Jerrett, J.R. de Bruyn, *Phys. Fluids A* **4**, 234 (1992)
4. M.A. Spaid, G.M. Homsy, *Phys. Fluids* **8**(2), 460 (1995)
5. A.L. Bertozzi, M.P. Brenner, *Phys. Fluids* **9**(3), 530 (1997), ISSN 1070-6631
6. S. Kalliadasis, *J. Fluid Mech.* **413**, 355 (2000)
7. M.H. Eres, L.W. Schwartz, R.V. Roy, *Phys. Fluids* **12**(6), 1278 (2000)
8. L. Kondic, J. Diez, *Physics of Fluids* **13**(11), 3168 (2001)
9. O. Pouliquen, J. Delour, S.B. Savage, *Nature* **386**, 816 (1997)
10. J. Zhou, B. Dupuy, A. Bertozzi, A. Hosoi, *Phys. Rev. Lett.* **94**(11), 117803 (2005)
11. B. Cook, A. Bertozzi, A. Hosoi, *SIAM J. Appl. Math.* **68**(3), 760 (2008)
12. M. Bowen, J. Sur, A.L. Bertozzi, R.P. Behringer, *Phys. D* **209**(1-4), 36 (2005), ISSN 0167-2789
13. D. Leighton, A. Acrivos, *J. Fluid Mech.* **181**, 415 (1987)
14. D. Leighton, Ph.D. thesis, Stanford Univ., Stanford, California (1985)
15. B.P. Cook (2007), under review.

¹ In [10] and [11] it is assumed that ϕ is independent of z due to the strength of this diffusion. This assumption is relaxed in [15].